# Combining Parameter-efficient Modules for Task-level Generalisation

**Anonymous EACL submission**

## Abstract

A modular design encourages neural models to disentangle and recombine different facets of knowledge to generalise more systematically to new tasks. In this work, we assume that each task is associated with a subset of latent skills from an (arbitrary size) inventory. In turn, each skill corresponds to a parameter-efficient (sparse / low-rank) model adapter. By jointly learning adapters and a routing function that allocates skills to each task, the full network is instantiated as the average of the parameters of active skills. We propose several inductive biases that encourage re-usage and composition of the skills, including variable-size skill allocation and a dual-speed learning rate. We evaluate our latent-skill model in two main settings: 1) multitask reinforcement learning for instruction following on 8 levels of the BabyAI platform; and 2) few-shot fine-tuning of language models on 160 NLP tasks of the CrossFit benchmark. We find that the modular design of our network enhances sample efficiency in reinforcement learning and few-shot generalisation in supervised learning, compared to a series of baselines. These include models where parameters are fully shared, task-specific, conditionally generated (HyperFormer), or sparse mixture-of-experts (TaskMoE).

## 1 Introduction

Task-level generalisation involves training a model on multiple tasks (in parallel or sequentially) and then performing zero-shot inference or few-shot adaptation on new tasks (Caruana, 1997; Ye et al., 2021). However, the training signals from different tasks may interfere with each other (McCloskey and Cohen, 1989) or lead to catastrophic forgetting of previous knowledge (French, 1999). Moreover, when the nature of the tasks varies between training and evaluation, models often struggle to generalise systematically (Hupkes et al., 2020).

A potential solution to these challenges consists in a modular design of neural architectures. In fact, these are endowed with an inductive bias towards updating and activating modules locally and asynchronously, thus preventing negative interference (Jacobs et al., 1991b). Additionally, by disentangling autonomous facets of knowledge (also known as *skills*) that are re-used and recombined in original ways for new tasks, modularity facilitates systematic generalisation (Alet et al., 2018; Ponti, 2021; Kingetsu et al., 2021, *inter alia*).

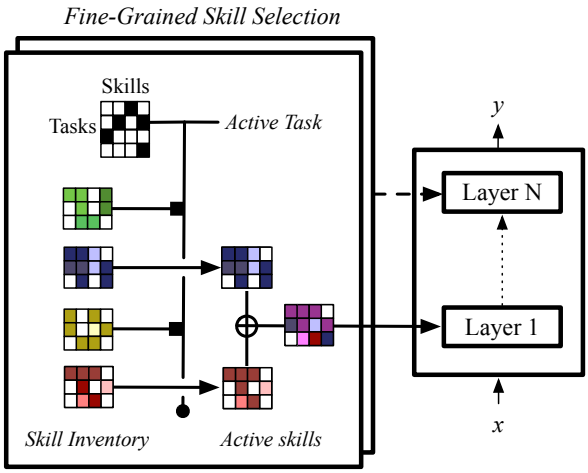


Figure 1: A diagram of our latent-skill model: 1) a row of the task–skill binary matrix is selected according to the active task; 2) the sparse (SFT) or low-rank (LoRA) adapters corresponding to active skills from a layer-specific inventory are combined; 3) the resulting combination is applied to the weights of a neural network, e.g. BART in our multi-task experiments.

Previous work on task-level generalisation focused on settings where the skills relevant for new tasks are already known *a priori* (Pfeiffer et al., 2020; Ansell et al., 2022). However, this requires expert knowledge, possibly with sub-optimal granularity and limited to a few domains. In alternative, mixture-of-expert (MoE) methods such as TaskMoE (Kudugunta et al., 2021a) learn a routing function that allocates modules to tasks end-to-end. However, MoEs mostly focus on scaling large language models trained from scratch, and their effec-

tiveness for out-of-domain generalisation is a moot point (Artetxe et al., 2021; Fedus et al., 2022).

In this work, we introduce a modular architecture that can efficiently adapt to new tasks, by virtue of a series of inductive biases that facilitate generalisation. The full model is shown in Figure 1. For each task, we learn a binary vector that specifies which skills (from a fixed inventory) are used to solve it. In the example, skills 2 and 4 are active. We implement each skill as a parameter-efficient adapter, either sparse (Ansell et al., 2022, SFT) or low-rank (Hu et al., 2021, LoRA). The parameters corresponding to every active skill (red and blue in the example) are then combined, by simple averaging. The resulting combination adapts a pretrained model, such as BART (Lewis et al., 2020), towards a specific task during multitask learning. The variable-size allocation of skills encourages their re-usage and re-combination in new tasks. To promote a coarse-to-fine dynamic where skill allocation is determined before skill-specific parameters, we explore a dual-speed learning rate for these two components (see Section 2.3).

We evaluate our model on reinforcement learning on BabyAI (Chevalier-Boisvert et al., 2019), a platform for instruction following in a simulated environment, and supervised learning on CrossFit (Ye et al., 2021), a benchmark recasting 160 NLP tasks as text-to-text generation problems. Compared to a series of competitive baselines, we obtain higher sample efficiency and higher performance in few-shot adaptation to held-out tasks. In particular, our latent-skill model surpasses non-modular methods for multi-task adaptation, such as HyperFormers (Karimi Mahabadi et al., 2021) and CA-MTL (Pilault et al., 2021), and mixture-of-experts methods such as TaskMoE (Kudugunta et al., 2021a).

Finally, we probe the learnt task–skill allocation matrix and illustrate how our method also enhances interpretability, as it discovers which pairs of tasks require common skills. The code is made available at `http://github.com/anonymous`.

## 2 A Latent-Skill Multitask Model

The goal of multitask learning in modelling a set of tasks $\mathcal{T} = (\mathcal{T}_1, \ldots, \mathcal{T}_{|\mathcal{T}|})$ is two-fold: 1) increasing sample efficiency on each seen task by borrowing statistical strength from the others; and 2) attaining systematic generalisation, the ability to adapt robustly to new tasks, possibly based on a few target-domain examples. In particular, in supervised learning, each task $\mathcal{T}_i$ is associated with a dataset $\mathcal{D}_i \triangleq \{(\mathbf{x}_1, \mathbf{y}_1), \ldots, (\mathbf{x}_n, \mathbf{y}_n)\}$ and a loss function $\mathcal{L}(\hat{\mathbf{y}}, \mathbf{y})$, where $\mathbf{x}$ is an input and $\mathbf{y}$ is an output. In reinforcement learning, each task is characterised by an initial state distribution $q(\mathbf{x}_1)$, a transition distribution $q(\mathbf{x}_{t+1} \mid \mathbf{x}_t, a_t)$, and a loss function $\mathcal{L}(\mathbf{x}_1, a_1, \ldots, \mathbf{x}_h, a_h) \rightarrow \mathbb{R}$,[1] where $\mathbf{x}$ is a state, $a$ is an action, and $h$ is the temporal horizon of each episode. Thus, each task defines a Markov Decision Process (MDP).

Fully sharing the parameters of a model across tasks (Stickland and Murray, 2019) may exhaust its capacity or create interference among the gradients from task-specific losses (Wang et al., 2021). These limitations can be countered by instead composing task-specific adapters (Pfeiffer et al., 2021) or softly sharing parameters (Ponti et al., 2021a; Karimi Mahabadi et al., 2021; Ansell et al., 2021). The first method leads to an explosion in parameter count, which grows with the number of tasks. Moreover, the second method suffers during few-shot adaptation to new tasks as the entangled (i.e., non-modular) knowledge may overfit the training distribution.

Instead, we posit that there exists a (possibly small) fixed inventory of skills $\mathcal{S} = (\mathcal{S}_1, \ldots, \mathcal{S}_{|\mathcal{S}|})$, where $|\mathcal{S}| \ll |\mathcal{T}|$. Each skill is an independent facet of knowledge that is reused across a subset of tasks. These assumptions guarantee both scalability and modularity. In particular, we seek to create a model that jointly learns which skills are active for which task, aggregates the corresponding skill parameters according to some deterministic function, and maximises the multitask log-likelihood:

$$\arg\max_{Z,\Phi} \sum_{\mathcal{T}_i} \sum_{(\mathbf{x},y)\in\mathcal{T}_i} \log p(y \mid \mathbf{x}, \boldsymbol{\vartheta}_i)\, p(Z)\, p(\Phi), \quad \text{where } \boldsymbol{\vartheta}_i = \delta(Z_i, \Phi, \boldsymbol{\vartheta}_0) \tag{1}$$

The learnable parameters, as shown in Figure 1, are: i) $Z$, which denotes the task–skill allocation matrix, representing a soft partition of skills across tasks; ii) $\Phi$, a tensor containing the parameters of each skill. As we explain in Section 2.4, these consist in either sparse or low-rank linear adapters. $\delta$ is a deterministic combination function that takes as input the task–skill allocation vector $Z_i$ for task $\mathcal{T}_i$, the skill parameters $\Phi$ and some shared parameters across tasks $\boldsymbol{\vartheta}_0$ and creates a task-dependent set

[1] This is the negative of the reward: $\mathcal{L}(\cdot) = -\mathcal{R}(\cdot)$.

of parameters $\boldsymbol{\vartheta}_i$, i.e. in our model, we use simple averaging of the active skills (see Figure 1). $\boldsymbol{\vartheta}_i$ is then used to predict the task label $y$ given the input $\mathbf{x}$. In what follows, we illustrate each component separately.

### 2.1 Soft Partitions

What is the best strategy to determine which skills are active for which task? The cognitively inspired notion of modularity at the level of structured inputs assumes that modules compete with each other for activation and updating (Bengio, 2017; Goyal et al., 2021). This intuition is translated in practice into a softmax across modules and top-$k$ selection, such as in mixture of experts (MoEs; Kudugunta et al., 2021a; Fedus et al., 2022). Nevertheless, we argue, modularity at the task level should reflect the fact that tasks fall into a hierarchy: more complex ones subsume simpler ones as sub-tasks. Hence, we allow for variable-size subsets of skills.

As a consequence, we assume that the matrix $Z \in \{0,1\}^{|\mathcal{T}|\times|\mathcal{S}|}$ representing task–skill allocations is a soft partition: each cell $z_{ij}$ is a binary scalar indicating if skill-specific parameters $\Phi_j$ are active for a certain task $\mathcal{T}_i$. However, being discrete, such a binary matrix is not differentiable and therefore cannot be learned end-to-end via gradient descent. Instead, we implement it as a collection of Bernoulli distributions continuously relaxed through a Gumbel-sigmoid (Maddison et al., 2017; Jang et al., 2017), which ensures stochasticity while allowing for differentiable sampling:

$$\hat{z}_{i,j} = \sigma\left[\log \frac{\sigma(z_{i,j})\, u}{(1-\sigma(z_{i,j}))\,(1-u)}^{1/\tau}\right]$$
$$u \sim \text{Uniform}(0,1). \quad (2)$$

In principle, either a coarse-grained soft partition can be learned globally for the entire neural network, or different fine-grained soft partitions can be assigned to each layer. We opt for the second alternative as it affords the model more flexibility and, foreshadowing, yields superior performance. Therefore, $Z$ and $\Phi$ are henceforth assumed to be layer-specific, although we will omit layer indexes in the notation for simplicity's sake.

### 2.2 Skill-specific Parameters

Given the matrix row $\hat{Z}_i$ for task $\mathcal{T}_i$ from Equation (2) and a matrix of skill-specific parameters $\Phi \in \mathbb{R}^{|\mathcal{S}|\times d}$, where $d$ is the dimension of the layer parameters, the aggregate of the parameters of active skills is superimposed to a base parameterisation $\boldsymbol{\vartheta}_0 \in \mathbb{R}^d$ shared across tasks. For instance, $\boldsymbol{\vartheta}_0$ may be either the initialisation from a pre-trained model or learned from scratch:

$$\boldsymbol{\vartheta}_i = \delta(Z_i, \Phi, \boldsymbol{\vartheta}_0) \triangleq \boldsymbol{\vartheta}_0 + \sum_{\mathcal{S}_j} \Phi_j \frac{\hat{z}_{i,j}}{\sum_{\mathcal{S}_j} \hat{z}_{i,j}}, \quad (3)$$

where $\boldsymbol{\vartheta}_i$ denote the parameters obtained by combining the active skills for the specific task $\mathcal{T}_i$. Note that we normalise the rows of the task–skill allocation matrix $\hat{Z}$ prior to composition because the variable number of active skills per task would otherwise affect the norm of the combined parameters $\boldsymbol{\vartheta}_i$, thus making training unstable.

### 2.3 Inductive Biases

A possible failure mode during training is a collapse into a highly entropic or non-sparse allocation matrix $\hat{Z}$, e.g., where all skills are active and skill-specific parameters remain general-purpose rather than specialising. Thus, we also provide an inductive bias to encourage the model to learn a low-entropy, highly-sparse allocation matrix.

In particular, we experiment with a dual-speed learning rate, setting its value for $Z$ higher than for $\Phi$. Intuitively, by accelerating learning of the soft partition matrix, to minimise the loss it becomes more convenient to discover better task–skill allocations over settling for general-purpose parameters that are agnostic with respect to the subset of active skills. This is reminiscent of the hypothesis that different kinds of knowledge require faster or slower rates of learning (Kahneman, 2011).

### 2.4 Parameter Efficiency

In order to keep the skills modular, each of them must correspond to a separate layer parameterisation. Nevertheless, this may lead to a significant increase in both time and space complexity. Thus, we explore parameter-efficient implementations of $\Phi$ that only add a negligible amount of parameters to the base model. In particular, we contemplate both sparse and low-rank approximations.

**Sparse Fine-Tuning** (SFT; Ansell et al., 2022) learns a highly sparse vector of differences $\Phi$ with respect to a base model $\boldsymbol{\vartheta}_0$. Its non-zero entries are identified by a binary matrix $M \in \{0,1\}^{|\mathcal{S}|\times d}$. For simplicity, we randomly draw $M$, as this was shown to perform almost on par with more sophisticated criteria without requiring a separate selection

phase (Ansell et al., 2022). SFT is agnostic with respect to the underlying neural architecture.

**Low-Rank Adapters** (LoRA; Hu et al., 2021) is another method for parameter-efficient fine-tuning designed specifically for Transformer architectures. It factorises each weight of the linear projections inside self-attention as a batched matrix multiplication between two low-rank tensors $A \in \mathbb{R}^{|\mathcal{S}| \times o \times r}$ and $B \in \mathbb{R}^{|\mathcal{S}| \times r \times i}$, where $r$ stands for the rank. In our model, each linear projection $f : \mathbb{R}^i \rightarrow \mathbb{R}^o$ is implemented as:

$$\mathbf{x}' = [W_0 + (\mathbf{z}^\top AB)]\mathbf{x} + \mathbf{b}_0 \quad (4)$$

where $\Phi \triangleq \text{flatten}(AB)$.

### 2.5 Baselines

We measure the performance of our SKILLED model, where we learn the skill–task allocation matrix $Z$ end-to-end, against these baselines, which derive from a certain configuration of $Z$:

- PRIVATE: each task has a separate model parameterisation. During few-shot adaptation, given that $\mathcal{T}_{train} \cap \mathcal{T}_{eval} = \emptyset$, this model cannot benefit from any transfer of information between training and evaluation tasks. This is equivalent to the special case where the task–skill allocation matrix is an identity matrix $Z = I$ of size $|\mathcal{T}| \times |\mathcal{T}|$ and $|\mathcal{S}| = |\mathcal{T}|$.
- SHARED: a shared skill is learnt on the training tasks and then fine-tuned for each evaluation task separately. This is equivalent to the special case where the task–skill allocation matrix is a matrix of ones $Z = \mathbf{1}$ of size $|\mathcal{T}| \times 1$ and $|\mathcal{S}| = 1$.
- EXPERT, where the task–skill allocation is contingent on expert knowledge about task relationships. Crucially, $Z$ is fixed *a priori* rather than being learned.

In addition, we compare our SKILLED method to a state-of-the-art baseline for multitask learning where parameters are softly shared, HYPER, based on HyperFormer (Karimi Mahabadi et al., 2021) and CA-MTL (Pilault et al., 2021). These methods generate adapters for the pre-trained model parameters with hyper-networks conditioned on task embeddings. Note that HYPER has a hidden connection with SKILLED, despite their apparent difference. In fact, we can draw an equivalence between i) binary skill vectors $\mathbf{z}$ and task embeddings; ii) the matrix of skill-specific parameters $\Phi$ and linear hyper-network weights. Crucially, in our case $\mathbf{z}$ is binary and modular, rather than continuous and entangled.

Finally, we compare SKILLED with TASK-MOE (Kudugunta et al., 2021a). This method relies on softmax and top-$k$ module selection, which does not favour module re-usage contrary to variable-size allocation. MoEs were originally conceived for scaling large language models trained from scratch, rather than model adaptation. To make HYPER and TASK-MOE compatible with the implementation of SKILLED in Equation (4), we implement their modules through LoRA rather their original formulations (Adapter layers and FFNs inside a Transformer layer, respectively).

## 3 Reinforcement Learning Experiments

### 3.1 Dataset

As a proof-of-concept experiment, we perform multitask reinforcement learning on the BabyAI platform (Chevalier-Boisvert et al., 2019). This benchmark consists in a series of increasingly complex levels, where an agent must execute a linguistic command by navigating a two-dimensional grid world and manipulating objects. Crucially, levels are procedurally generated to reflect different subsets of skills (e.g., PICKUP, UNLOCK, *et cetera*). This enables us to test our model in a controlled setting where performance based on learned skills can be compared with 'ground truth' skills. In particular, we focus on a similar subset of 8 levels as Hui et al. (2020).

### 3.2 Experimental Setup

The neural architecture adheres to the best model reported in Hui et al. (2020), BOW_ENDPOOL_RES. It encodes the linguistic input through a Gated Recurrent Unit (GRU; Cho et al., 2014) and the visual input through a convolutional network (CNN). These two streams from different modalities are then merged into a single representation through FiLM (Perez et al., 2018). This component performs a feature-wise affine transformation of the CNN output conditioned on the GRU output.

Afterwards, a Long Short-Term Memory network (LSTM; Hochreiter and Schmidhuber, 1997), a recurrent module keeping track of the agent state trajectory, receives the multimodal representation and returns the current hidden state. This in turn is fed into two distinct MLPs, an actor and a critic

(Sutton, 1984). The actor yields a distribution over actions, whereas the critic a reward baseline for the current state. In our experiments, each row of the matrix $\Phi$ corresponds to a possible parameterisation for all these components.

To determine *a priori* a skill–task allocation for the EXPERT baseline, we harness the information about the skills employed to procedurally generate each level by Chevalier-Boisvert et al. (2019, p. 6). For the SKILLED model, we set $|\mathcal{S}| = 9$ similarly to EXPERT. This allows us to compare learned skills and 'ground-truth' skills from an inventory of identical size. As a parameter-efficient implementation of $\Phi$, we employ SFT (Ansell et al., 2022) with a sparsity of $90\%$. For all model variants, $\boldsymbol{\vartheta}_0$ and $\Phi$ are both initialised from a Kaiming uniform (He et al., 2015) and learnable. During training, we sample levels uniformly. The full specification of hyper-parameters is available in Appendix A.

### 3.3 Results

We now measure if our latent-skill model facilitates sample efficiency, which following Chevalier-Boisvert et al. (2019) is defined as the number of episodes required for an agent to reach a success rate greater than $0.99$.[2] Success in turn is defined as executing an instruction in a number of steps $n < n_{\max}$, where the threshold again depends on the level complexity.

We plot our results in Figure 2. Firstly, models sharing information across tasks (either fully or mediated by skills) enjoy higher sample efficiency than assigning disjoint parameters for each task (PRIVATE), as they can borrow statistical strength from each other. Crucially, among information-sharing models, dual-speed SKILLED (where knowledge is modular) surpasses SHARED (where knowledge is entangled among tasks). Thus, considering a task as a collection of fine-grained skills that can be separated and reused is the most effective way of sharing information. Finally, results surprisingly show that learning a task–skill allocation matrix end-to-end (SKILLED) is more beneficial than leveraging the ground-truth task–skill decomposition used to create the BabyAI levels (EXPERT). This highlights the fact that different tasks might mutually benefit in ways that go beyond what is posited *a priori* by experts, and that our proposed approach can successfully uncover and exploit such task synergies.

[2]Success rate alone is insufficient as a performance metric as most models can solve all the levels if given enough time.

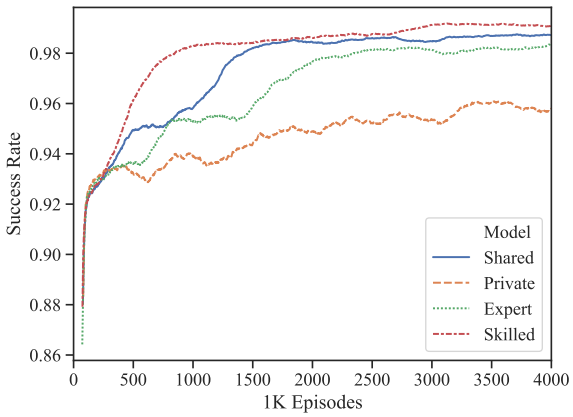


Figure 2: Sample efficiency (success rate vs. number of episodes) for different multitask models across 8 levels of BabyAI. Moving average with window of 100.

Moreover, we run ablations to study the impact of the inductive biases and the parameter-efficient implementation. We compare the SKILLED model in the standard setup (with dual-speed learning rates and sparse skill-specific parameters) with other variants (with a single learning rate or with fully dense skill-specific parameters) in terms of sample efficiency in Table 3 in Appendix B. We find that assigning the same learning rate to every model component drastically slows convergence to an almost-perfect success rate. In addition, employing fully dense skill-specific parameters increases sample efficiency only to a limited degree (~1.9M). Thus, we can verify that parameter sparsification offers an effective trade-off between performance and space complexity.

## 4 Supervised Learning Experiments

### 4.1 Dataset

In order to measure the benefits of a modular design for systematic generalisation to new tasks, we run a second set of experiments on CrossFit (Ye et al., 2021), a benchmark including 160 diverse natural language processing tasks in English sourced from Huggingface Datasets (Lhoest et al., 2021). The tasks in CrossFit are all converted into a unified text-to-text format inspired by Raffel et al. (2020). Moreover, they are partitioned into three disjoint subsets. First, a model is pre-trained in a multitask fashion on training tasks $\mathcal{T}_{train}$. Afterwards, it is adapted to each evaluation task from $\mathcal{T}_{eval}$ in a few-shot learning setting. Hyper-parameter are tuned on the held-out set $\mathcal{T}_{dev}$.

| TASK | Metric | Ye et al. (2021) | Shared | Private | Expert | Hyper-Former | Task-MoE | Skilled |
|---|---|---|---|---|---|---|---|---|
| AG-NEWS | C–F1 | 84.6 ± 1.4 | 59.6 ± 21.1 | 74.7 ± 10.2 | 47.0 ± 9.9 | 64.6 ± 13.4 | 79.2 ± 13.1 | 81.2 ± 8.0 |
| AI2-ARC | Acc | 22.8 ± 1.9 | 23.7 ± 2.4 | 20.3 ± 0.8 | 28.3 ± 3.7 | 23.8 ± 6.7 | 19.6 ± 5.6 | 22.3 ± 3.4 |
| AMAZON-POLARITY | C–F1 | 92.2 ± 0.6 | 92.4 ± 2.8 | 94.4 ± 0.4 | 57.4 ± 3.1 | 93.8 ± 1.5 | 87.3 ± 14.0 | 93.7 ± 0.9 |
| BSN-NPI-LICENSOR | Acc | 99.9 ± 0.2 | 99.9 ± 0.0 | 99.9 ± 0.0 | 99.9 ± 0.0 | 99.9 ± 0.0 | 99.9 ± 0.0 | 99.9 ± 0.2 |
| BSN-NPI-SCOPE | Acc | 85.7 ± 13.0 | 99.8 ± 0.3 | 99.6 ± 0.9 | 99.9 ± 0.2 | 99.9 ± 0.0 | 99.9 ± 0.0 | 99.9 ± 0.2 |
| BREAK-QDMR | EM | 4.8 ± 0.4 | 4.1 ± 0.5 | 1.9 ± 1.7 | 4.1 ± 0.9 | 3.8 ± 1.2 | 4.2 ± 0.8 | 4.9 ± 0.6 |
| CIRCA | C–F1 | 42.3 ± 7.8 | 44.3 ± 7.5 | 22.2 ± 6.3 | 13.0 ± 7.0 | 25.0 ± 6.3 | 39.9 ± 9.3 | 45.9 ± 5.7 |
| CRAWL-DOMAIN | EM | 20.7 ± 2.0 | 40.9 ± 2.2 | 36.2 ± 6.3 | 37.1 ± 5.3 | 34.9 ± 3.8 | 44.5 ± 2.7 | 39.0 ± 4.2 |
| ETHOS-DISABILITY | C–F1 | 75.3 ± 2.2 | 66.9 ± 11.8 | 64.7 ± 12.1 | 59.2 ± 15.8 | 79.4 ± 3.9 | 66.8 ± 5.2 | 72.2 ± 5.2 |
| ETHOS-SEXUAL | C–F1 | 59.7 ± 5.7 | 62.4 ± 8.4 | 71.2 ± 9.8 | 40.3 ± 11.4 | 76.8 ± 10.0 | 76.7 ± 14.4 | 86.1 ± 2.6 |
| FREEBASE-QA | EM | 1.3 ± 0.1 | 0.7 ± 0.2 | 0.2 ± 0.1 | 1.3 ± 0.5 | 1.6 ± 0.8 | 0.7 ± 0.6 | 0.7 ± 0.3 |
| GLUE-COLA | M-Corr | 3.5 ± 6.7 | 12.9 ± 5.5 | 9.1 ± 6.3 | 7.6 ± 5.6 | 6.8 ± 4.2 | 10.8 ± 10.7 | 7.1 ± 5.3 |
| GLUE-QNLI | Acc | 74.7 ± 2.9 | 75.5 ± 3.6 | 57.1 ± 7.7 | 56.6 ± 19.7 | 73.9 ± 3.2 | 75.0 ± 3.3 | 78.1 ± 1.6 |
| HATEXPLAIN | C–F1 | 44.9 ± 2.5 | 33.1 ± 8.2 | 26.5 ± 7.8 | 11.9 ± 4.0 | 23.2 ± 6.2 | 41.9 ± 4.2 | 32.6 ± 13.6 |
| QUOREF | QA-F1 | 41.2 ± 1.6 | 46.0 ± 4.4 | 36.3 ± 4.6 | 48.4 ± 4.3 | 41.7 ± 6.5 | 44.3 ± 3.1 | 47.3 ± 3.5 |
| RACE-HIGH | Acc | 30.5 ± 1.5 | 34.0 ± 2.7 | 28.5 ± 1.4 | 38.5 ± 2.0 | 30.8 ± 1.9 | 30.2 ± 3.2 | 34.8 ± 2.0 |
| SUPERGLUE-RTE | Acc | 60.4 ± 3.6 | 60.6 ± 2.9 | 49.7 ± 5.1 | 51.7 ± 4.8 | 60.9 ± 3.8 | 59.5 ± 5.2 | 60.4 ± 5.9 |
| TWEET-EVAL-IRONY | C–F1 | 55.2 ± 3.6 | 52.1 ± 8.0 | 50.1 ± 14.2 | 25.6 ± 8.9 | 38.4 ± 6.0 | 51.8 ± 12.6 | 57.2 ± 2.4 |
| WIKI-SPLIT | Rouge-L | 79.3 ± 0.5 | 80.1 ± 0.6 | 80.3 ± 0.6 | 79.2 ± 0.8 | 79.2 ± 0.7 | 80.0 ± 0.7 | 80.6 ± 0.3 |
| YELP-POLARITY | C–F1 | 71.8 ± 21.1 | 88.3 ± 14.9 | 65.0 ± 20.5 | 53.9 ± 12.7 | 95.0 ± 0.9 | 76.2 ± 17.6 | 94.5 ± 1.1 |
| ALL | - | 52.5 ± 1.5 | 53.9 ± 1.7 | 49.4 ± 1.6 | 43.0 ± 2.2 | 52.7 ± 1.0 | 54.9 ± 1.4 | **56.9** ± 1.2 |

Table 1: Few-shot adaptation results of SKILLED and five baselines, including the original model from Ye et al. (2021), on 20 evaluation tasks of CrossFit (Ye et al., 2021). For the full name of the metrics, refer to Section 4.1.

We adopt the partition 1 (called RANDOM) from Ye et al. (2021), where $|\mathcal{T}_{train}| = 120$, $|\mathcal{T}_{dev}| = |\mathcal{T}_{eval}| = 20$, and tasks are split randomly. This is the most comprehensive partition and most suited for general-purpose models, as it includes all types of tasks. Every task is associated with 5 different few-shot data splits for train $\mathcal{D}_{train}$ and development $\mathcal{D}_{dev}$ and 1 larger data split for evaluation $\mathcal{D}_{eval}$. During multitask pre-training, we concatenate all $\mathcal{D}_{train}$ and $\mathcal{D}_{dev}$ from $\mathcal{T}_{train}$. During few-shot adaptation, for each task in $\mathcal{T}_{eval}$ we use each $\mathcal{D}_{train}$ and $\mathcal{D}_{dev}$ separately in 5 distinct runs and evaluate on $\mathcal{D}_{eval}$. We measure the performance of a model with 7 evaluation metrics according to the type of task: C[lassification]-F1, Acc[uracy], QA-F1, E[xact] M[atch], Rouge-L, M[atthew]-Corr[elation], and P[earson]-Corr[elation].

## 4.2 Experimental Setup

As pre-trained weights $\vartheta_0$ and architecture for conditional text generation, we choose BART Large (Lewis et al., 2020), a 24-layer Transformer-based encoder–decoder. We use LoRA (Hu et al., 2021) to implement skill-specific parameters efficiently, as it was explicitly designed for the Transformer architecture (cf. Section 2.4). While $\vartheta_0$ remains frozen, $A$ matrices in $\Phi$ are initialised to zero matrices following Hu et al. (2021).

As a source of expert knowledge for the EXPERT baseline, we associate each task to a unique skill corresponding to one of the 4 task types of Ye et al. (2021, p. 20)'s taxonomy: question answering, conditional text generation, classification, or other (e.g., regression). The skill inventory size of 8 for SKILLED was chosen among $\{2, 4, 8, 16, 32\}$ based on validation. We set the embedding size $e$ and hidden size $h$ of HYPER to an identical value to ensure a fair comparison. Both SKILLED and HYPER therefore increase the parameter count by $\sim 0.78\%$ per skill and task embedding dimension, respectively. We provide more information on the hyper-parameter configuration in Appendix A.

## 4.3 Results

**Few-shot Adaptation to New Tasks** In the few-shot adaptation setting, our goal is to evaluate the capability of the model to quickly generalise to new tasks unseen during training. This is the most realistic setting as tasks encountered by models deployed 'in the wild' will be characterised by different distributions or involve different input / output spaces. Performance in terms of task-specific metrics is reported in Table 1 for the 20 evaluation tasks individually and on average.

Crucially, results show that SKILLED outperforms alternative formulations of the task–skill allocation matrix, such as SHARED, PRIVATE and EXPERT. Importantly, we note that SKILLED also surpasses HYPER by a sizeable margin despite the two models having comparable parameter counts.

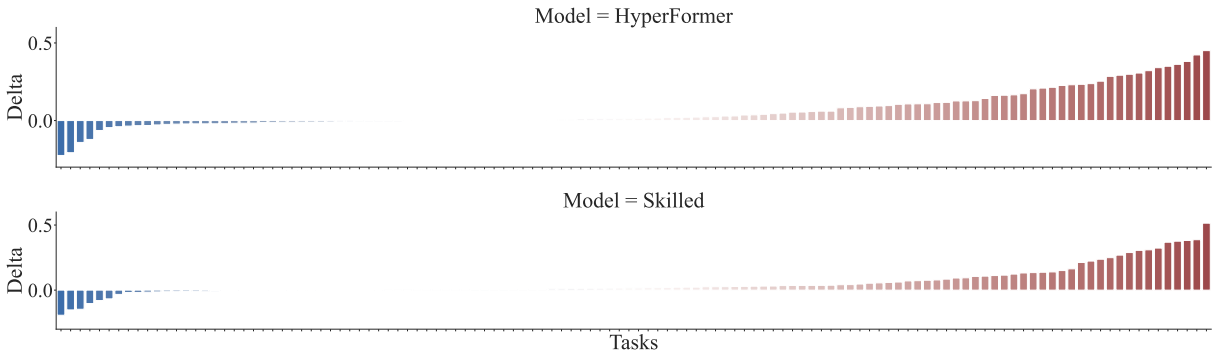


Figure 3: Delta in performance in terms of task-specific metrics between SKILLED (bottom) and HYPER (top) on the one hand and SHARED on the other, across 120 CrossFit tasks seen during multitask pre-training.

This points to the fact that explicitly modularising knowledge learnt during multitask training is important for systematic adaptation to unseen tasks, whereas entangled knowledge is more brittle to distribution shifts in cross-task transfer. Similarly, the average performance of SKILLED is significantly higher that TASK-MOE, which illustrates the importance of variable-size module allocation. Also, it demonstrates that modularity holds promise not only for scaling large language models, but also as a strategy to favour generalisation. Finally, we corroborate the soundness of our experiment setup by reproducing the results of Ye et al. (2021).[3]

**Multitask Evaluation on Seen Tasks** Moreover, to ensure that modularity does not adversely affect in-domain performance, we evaluate models on the test sets of seen tasks after multitask training. In Figure 3, we report the delta in performance in terms of task-specific metrics between two models (SKILLED on top, HYPER on the bottom) and a baseline (SHARED) for the 120 training tasks. Both models yield positive gains for most tasks over SHARED. Most importantly, SKILLED achieves a performance (48.95 on average) comparable to HYPER (49.37 on average), therefore confirming that explicit modularisation can be as effective as conditional parameter generation when evaluated on seen tasks, but also engenders vast improvements on held-out tasks.

**In-Depth Analysis of Learned Skills** Finally, we run an in-depth analysis of the task–skill allocation matrices $Z$ learned by SKILLED. We visualise its posterior for $|\mathcal{S}| = 4$ in Figure 4 and measure metrics related to discreteness, sparsity, and diversity in Appendix D. Overall, these results demonstrate that a quasi-binary, highly-sparse, and non-trivial allocation matrix can be successfully learned in an end-to-end fashion even with simple inductive biases such as a dual-speed learning rate.

Crucially, learning a skill allocation also facilitates interpreting black-box multitask models. In fact, the structure of $Z$ corresponds to an explicit hierarchy of tasks, where simpler ones are subsumed by more complex ones, and similar tasks can be grouped into the same category if they share the same subset of skills. We plot this hierarchy as a dendrogram in Figure 5. For instance, most GLUE tasks (Wang et al., 2018) are grouped together as they are all focused on natural language understanding: for instance, they require skill 1 (COLA), 2 (MRPC, RTE, SST2, WNLI), or both 1 and 2 (MNLI, QQP).

## 5 Related Work

**Modular Networks** Modularising neural networks has long been sought as a way to achieve better generalisation to unseen inputs (Jacobs et al., 1991b; Andreas et al., 2016; Kirsch et al., 2018), tasks (Jacobs et al., 1991a; Alet et al., 2018), and recently to improve continual learning (Ostapenko et al., 2021), to be more robust to changes in the environment (Goyal et al., 2021) and for sequence generation (Zhang et al., 2022).

In routing networks (Rosenbaum et al., 2019), a learnable router decides the order in which modules are applied to the input. Learning the structure of this composition has been achieved using an external parser (Andreas et al., 2016) or by sampling structures with simulated annealing (Alet et al., 2018). In mixture of experts (MoE), the system selects a soft subset of modules depending on the input to be processed (Jacobs et al., 1991b; Shazeer

[3]Note that in Ye et al. (2021) the pre-trained model is BART Small and all parameters are fine-tuned. Hence, these results are not directly comparable.

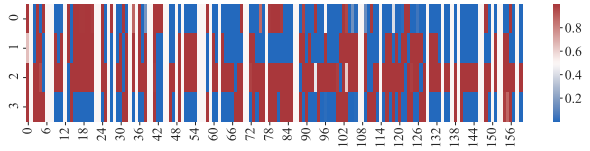

Figure 4: Posterior over $Z$ in SKILLED for $|\mathcal{S}| = 4$.

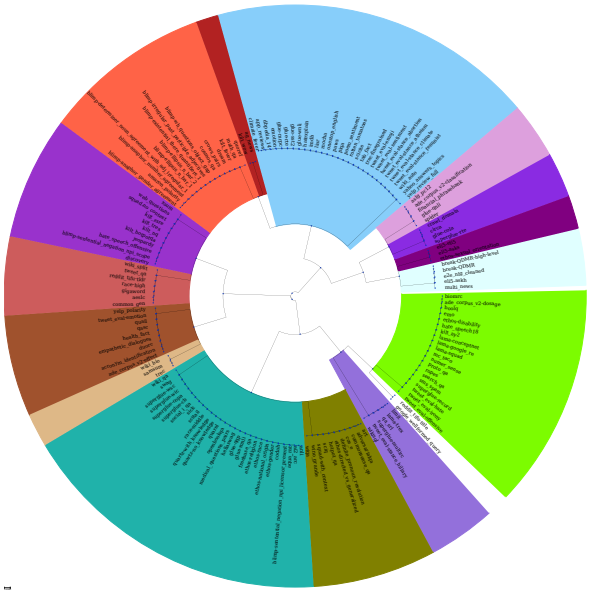

Figure 5: Task partitions for $|\mathcal{S}| = 4$, which corresponds to $2^{|\mathcal{S}|} = 16$ possible subsets of skills.

et al., 2017). MoEs can be interpreted invoking the theory of independent mechanisms (Parascandolo et al., 2018) that Goyal et al. (2021) further extend to handle sequential problems. Sun et al. (2020) share subsets of parameters among sparse sub-networks corresponding to different tasks. Within NLP, Fedus et al. (2021) uses a MoE architecture to scale large language model pre-training to trillions of parameters.

Our model conditions the computation on the task rather than on task inputs. Attempts to enforce parameter reuse and modularity for multi-task learning include (Rajendran et al., 2017; Ponti et al., 2021a; Kingetsu et al., 2021; Kudugunta et al., 2021b). Rajendran et al. (2017) learn separate modules for each task and then learn how to reuse those modules for a new task. Kudugunta et al. (2021b) uses a set of modules for each task in a multi-lingual translation setting. Our approach does not assume a set of modules for each task but instead decomposes a task into a set of skills themselves reusable across tasks.

**Multitask NLP** Joint multitask learning in NLP proved an effective strategy for improving model performance in low-resource tasks and for quickly adapting to new tasks (Ruder et al., 2019; Min et al., 2021; Wei et al., 2021; Aribandi et al., 2021; Sanh et al., 2022), languages (Ponti et al., 2019), and modalities (Bugliarello et al., 2022). Liu et al. (2019) trained a shared model for all GLUE tasks and achieved impressive performance on GLUE. Pfeiffer et al. (2021) share information across task-specific parameters while alleviating negative task interference.

In our experiments we parameterise each skill with two kinds of adapters: either SFT (Ansell et al., 2022) or LoRA (Hu et al., 2021). Recently, Karimi Mahabadi et al. (2021) and Pilault et al. (2021) ensure cross-task information sharing by using a hyper-network to generate adapters from task embeddings. Differently, our task-specific parameters are composed of a set of skills from a shared inventory, which makes our approach modular and more scalable.

Several multitask approaches specifically target adaptation to new tasks, such as meta-learning approaches (Alet et al., 2018; Rusu et al., 2019; Ponti et al., 2021b; Garcia et al., 2021; Ostapenko et al., 2021). In our paper, we efficiently achieve few-shot task adaptation by inferring the skill allocation for new tasks and fine-tuning skill parameters initialised from multitask learning.

## 6 Conclusions

We argued that a modular design is crucial to ensure that neural networks can learn from a few examples and generalise robustly across tasks by recombining autonomous facets of knowledge. To this end, we proposed a model where a subset of latent, discrete skills from a fixed inventory is allocated to each task in an end-to-end fashion. The task-specific instantiation of a neural network is then obtained by combining efficient parameterisations of the active skills, such as sparse or low-rank adapters. We evaluate the sample efficiency of our model on multitask instruction following through reinforcement learning and its few-shot adaptability on multitask text-to-text generation through supervised learning. In both experiments, we surpass competitive baselines such as conditional parameter generation (HyperFormer) and mixture of experts (Task-MoE). Finally, we show that modularity helps interpret multi-task models by inferring explicit relationships between tasks according to the skills they share.

## Limitations

Firstly, the kind of knowledge captured by individual skills is not fully interpretable. In terms of task–skill allocation, while some patterns based on task type and textual domain emerge from the clusters of Figure 5, it remains unclear how to systematically probe this information. Moreover, in terms of skill-specific parameters, it is hard to measure the diversity among learned skills. In fact, due to the under-specification of neural networks, different configurations in the parameter space may in fact correspond to the same function.

Secondly, few-shot adaptation in our experiments is based on the assumption that the skill inventory is fixed. Therefore, the model is compelled to recombine and possibly fine-tune old skills. Instead, each unseen task should involve a combination of newly discovered and previously honed skills. In the future, a possible extension of our method for continuous learning should adopt this more natural assumption.

Finally, we explore only a subset of the problems where different skills can be combined. In addition to instruction following and conditional text generation, our results should be replicated also in multilingual and multimodal benchmarks (Bugliarello et al., 2022, *inter alia*).

## References


Ferran Alet, Tomas Lozano-Perez, and Leslie P. Kaelbling. 2018. Modular meta-learning. In *Proceedings of The 2nd Conference on Robot Learning*, pages 856–868.

Jacob Andreas, Marcus Rohrbach, Trevor Darrell, and Dan Klein. 2016. Neural module networks. In *Proceedings of the IEEE Conference on Computer Vision and Pattern Recognition (CVPR)*, pages 39–48.

Alan Ansell, Edoardo Maria Ponti, Anna Korhonen, and Ivan Vulić. 2022. Composable sparse fine-tuning for cross-lingual transfer. In *Proceedings of the 60th Annual Meeting of the Association for Computational Linguistics*.

Alan Ansell, Edoardo Maria Ponti, Jonas Pfeiffer, Sebastian Ruder, Goran Glavaš, Ivan Vulić, and Anna Korhonen. 2021. MAD-G: Multilingual adapter generation for efficient cross-lingual transfer. In *Findings of the Association for Computational Linguistics: EMNLP 2021*, pages 4762–4781.

Vamsi Aribandi, Yi Tay, Tal Schuster, Jinfeng Rao, Huaixiu Steven Zheng, Sanket Vaibhav Mehta, Honglei Zhuang, Vinh Q. Tran, Dara Bahri, Jianmo Ni, Jai Gupta, Kai Hui, Sebastian Ruder, and Donald Metzler. 2021. ExT5: Towards extreme multi-task scaling for transfer learning. *arXiv preprint arXiv:2111.10952*.

Mikel Artetxe, Shruti Bhosale, Naman Goyal, Todor Mihaylov, Myle Ott, Sam Shleifer, Xi Victoria Lin, Jingfei Du, Srinivasan Iyer, Ramakanth Pasunuru, et al. 2021. Efficient large scale language modeling with mixtures of experts. *arXiv preprint arXiv:2112.10684*.

Yoshua Bengio. 2017. The consciousness prior. *arXiv preprint arXiv:1709.08568*.

Emanuele Bugliarello, Fangyu Liu, Jonas Pfeiffer, Siva Reddy, Desmond Elliott, Edoardo Maria Ponti, and Ivan Vulić. 2022. IGLUE: A benchmark for transfer learning across modalities, tasks, and languages. *arXiv preprint arXiv:2201.11732*.

Rich Caruana. 1997. Multitask learning. *Machine learning*, 28(1):41–75.

Maxime Chevalier-Boisvert, Dzmitry Bahdanau, Salem Lahlou, Lucas Willems, Chitwan Saharia, Thien Huu Nguyen, and Yoshua Bengio. 2019. BabyAI: First steps towards grounded language learning with a human in the loop. In *International Conference on Learning Representations*.

Kyunghyun Cho, Bart van Merriënboer, Dzmitry Bahdanau, and Yoshua Bengio. 2014. On the properties of neural machine translation: Encoder–decoder approaches. In *Proceedings of SSST-8, Eighth Workshop on Syntax, Semantics and Structure in Statistical Translation*, pages 103–111.

William Fedus, Jeff Dean, and Barret Zoph. 2022. A review of sparse expert models in deep learning. *arXiv preprint arXiv:2209.01667*.

William Fedus, Barret Zoph, and Noam Shazeer. 2021. Switch Transformers: Scaling to trillion parameter models with simple and efficient sparsity. *arXiv preprint arXiv:2101.03961*.

Robert M French. 1999. Catastrophic forgetting in connectionist networks. *Trends in cognitive sciences*, 3(4):128–135.

Jezabel R Garcia, Federica Freddi, Feng-Ting Liao, Jamie McGowan, Tim Nieradzik, Da-shan Shiu, Ye Tian, and Alberto Bernacchia. 2021. Meta-learning with MAML on trees. *arXiv preprint arXiv:2103.04691*.

Anirudh Goyal, Alex Lamb, Jordan Hoffmann, Shagun Sodhani, Sergey Levine, Yoshua Bengio, and Bernhard Schölkopf. 2021. Recurrent independent mechanisms. In *International Conference on Learning Representations*.

Kaiming He, Xiangyu Zhang, Shaoqing Ren, and Jian Sun. 2015. Delving deep into rectifiers: Surpassing human-level performance on imagenet classification.

In *Proceedings of the IEEE international conference on computer vision*, pages 1026–1034.

Sepp Hochreiter and Jürgen Schmidhuber. 1997. Long short-term memory. *Neural computation*, 9(8):1735–1780.

Edward J Hu, Yelong Shen, Phillip Wallis, Zeyuan Allen-Zhu, Yuanzhi Li, Shean Wang, Lu Wang, and Weizhu Chen. 2021. LoRA: Low-rank adaptation of large language models. *arXiv preprint arXiv:2106.09685*.

David Yu-Tung Hui, Maxime Chevalier-Boisvert, Dzmitry Bahdanau, and Yoshua Bengio. 2020. BabyAI 1.1. *arXiv preprint arXiv:2007.12770*.

Dieuwke Hupkes, Verna Dankers, Mathijs Mul, and Elia Bruni. 2020. Compositionality decomposed: How do neural networks generalise? *Journal of Artificial Intelligence Research*, 67:757–795.

Robert A Jacobs, Michael I Jordan, and Andrew G Barto. 1991a. Task decomposition through competition in a modular connectionist architecture: The what and where vision tasks. *Cognitive science*, 15(2):219–250.

Robert A Jacobs, Michael I Jordan, Steven J Nowlan, and Geoffrey E Hinton. 1991b. Adaptive mixtures of local experts. *Neural computation*, 3(1):79–87.

Eric Jang, Shixiang Gu, and Ben Poole. 2017. Categorical reparameterization with Gumbel-softmax. In *International Conference on Learning Representations*.

Daniel Kahneman. 2011. *Thinking, fast and slow*. Macmillan.

Rabeeh Karimi Mahabadi, Sebastian Ruder, Mostafa Dehghani, and James Henderson. 2021. Parameter-efficient multi-task fine-tuning for Transformers via shared hypernetworks. In *Proceedings of the 59th Annual Meeting of the Association for Computational Linguistics and the 11th International Joint Conference on Natural Language Processing*, pages 565–576.

Hiroaki Kingetsu, Kenichi Kobayashi, and Taiji Suzuki. 2021. Neural network module decomposition and recomposition. *arXiv preprint arXiv:2112.13208*.

Diederik P Kingma and Jimmy Ba. 2015. Adam: A method for stochastic optimization. In *International Conference on Learning Representations*.

Louis Kirsch, Julius Kunze, and David Barber. 2018. Modular networks: Learning to decompose neural computation. *Advances in Neural Information Processing Systems*, 31.

Sneha Kudugunta, Yanping Huang, Ankur Bapna, Maxim Krikun, Dmitry Lepikhin, Minh-Thang Luong, and Orhan Firat. 2021a. Beyond distillation: Task-level mixture-of-experts for efficient inference. In *Findings of the Association for Computational Linguistics: EMNLP 2021*, pages 3577–3599, Punta Cana, Dominican Republic. Association for Computational Linguistics.

Sneha Kudugunta, Yanping Huang, Ankur Bapna, Maxim Krikun, Dmitry Lepikhin, Minh-Thang Luong, and Orhan Firat. 2021b. Beyond distillation: Task-level mixture-of-experts for efficient inference. In *Findings of the Association for Computational Linguistics: EMNLP 2021*, pages 3577–3599.

Mike Lewis, Yinhan Liu, Naman Goyal, Marjan Ghazvininejad, Abdelrahman Mohamed, Omer Levy, Veselin Stoyanov, and Luke Zettlemoyer. 2020. BART: Denoising sequence-to-sequence pre-training for natural language generation, translation, and comprehension. In *Proceedings of the 58th Annual Meeting of the Association for Computational Linguistics*, pages 7871–7880.

Quentin Lhoest, Albert Villanova del Moral, Yacine Jernite, Abhishek Thakur, Patrick von Platen, Suraj Patil, Julien Chaumond, Mariama Drame, Julien Plu, Lewis Tunstall, Joe Davison, Mario Šaško, Gunjan Chhablani, Bhavitvya Malik, Simon Brandeis, Teven Le Scao, Victor Sanh, Canwen Xu, Nicolas Patry, Angelina McMillan-Major, Philipp Schmid, Sylvain Gugger, Clément Delangue, Théo Matussière, Lysandre Debut, Stas Bekman, Pierric Cistac, Thibault Goehringer, Victor Mustar, François Lagunas, Alexander Rush, and Thomas Wolf. 2021. Datasets: A community library for natural language processing. In *Proceedings of the 2021 Conference on Empirical Methods in Natural Language Processing: System Demonstrations*, pages 175–184.

Xiaodong Liu, Pengcheng He, Weizhu Chen, and Jianfeng Gao. 2019. Multi-task deep neural networks for natural language understanding. In *Proceedings of the 57th Annual Meeting of the Association for Computational Linguistics*, pages 4487–4496.

Chris J Maddison, Andriy Mnih, and Yee Whye Teh. 2017. The concrete distribution: A continuous relaxation of discrete random variables. In *Proceedings of the International Conference on Learning Representations 2017*.

Michael McCloskey and Neal J Cohen. 1989. Catastrophic interference in connectionist networks: The sequential learning problem. In *Psychology of learning and motivation*, volume 24, pages 109–165. Elsevier.

Sewon Min, Mike Lewis, Luke Zettlemoyer, and Hannaneh Hajishirzi. 2021. MetaICL: Learning to learn in context. *arXiv preprint arXiv:2110.15943*.

Oleksiy Ostapenko, Pau Rodriguez, Massimo Caccia, and Laurent Charlin. 2021. Continual learning via local module composition. *Advances in Neural Information Processing Systems*, 34.

Giambattista Parascandolo, Niki Kilbertus, Mateo Rojas-Carulla, and Bernhard Schölkopf. 2018. Learning independent causal mechanisms. In *International Conference on Machine Learning*, pages 4036–4044.

Ethan Perez, Florian Strub, Harm De Vries, Vincent Dumoulin, and Aaron Courville. 2018. FiLM: Visual reasoning with a general conditioning layer. In *Proceedings of the AAAI Conference on Artificial Intelligence*, volume 32.

Jonas Pfeiffer, Aishwarya Kamath, Andreas Rücklé, Kyunghyun Cho, and Iryna Gurevych. 2021. AdapterFusion: Non-destructive task composition for transfer learning. In *Proceedings of the 16th Conference of the European Chapter of the Association for Computational Linguistics*, pages 487–503.

Jonas Pfeiffer, Ivan Vulić, Iryna Gurevych, and Sebastian Ruder. 2020. MAD-X: An Adapter-based framework for multi-task cross-lingual transfer. In *Proceedings of the 2020 Conference on Empirical Methods in Natural Language Processing (EMNLP)*, pages 7654–7673.

Jonathan Pilault, Amine El hattami, and Christopher Pal. 2021. Conditionally adaptive multi-task learning: Improving transfer learning in NLP using fewer parameters & less data. In *International Conference on Learning Representations*.

Edoardo Ponti. 2021. *Inductive Bias and Modular Design for Sample-Efficient Neural Language Learning*. Ph.D. thesis, University of Cambridge.

Edoardo M Ponti, Ivan Vulić, Ryan Cotterell, Marinela Parovic, Roi Reichart, and Anna Korhonen. 2021a. Parameter space factorization for zero-shot learning across tasks and languages. *Transactions of the Association for Computational Linguistics*.

Edoardo Maria Ponti, Rahul Aralikatte, Disha Shrivastava, Siva Reddy, and Anders Søgaard. 2021b. Minimax and Neyman–Pearson meta-learning for outlier languages. In *Findings of the Association for Computational Linguistics: ACL-IJCNLP 2021*, pages 1245–1260.

Edoardo Maria Ponti, Helen O'Horan, Yevgeni Berzak, Ivan Vulić, Roi Reichart, Thierry Poibeau, Ekaterina Shutova, and Anna Korhonen. 2019. Modeling language variation and universals: A survey on typological linguistics for natural language processing. *Computational Linguistics*, 45(3):559–601.

Colin Raffel, Noam Shazeer, Adam Roberts, Katherine Lee, Sharan Narang, Michael Matena, Yanqi Zhou, Wei Li, and Peter J Liu. 2020. Exploring the limits of transfer learning with a unified text-to-text transformer. *Journal of Machine Learning Research*, 21:1–67.

Janarthanan Rajendran, P Prasanna, Balaraman Ravindran, and Mitesh M Khapra. 2017. Attend, adapt and transfer: Attentive deep architecture for adaptive transfer from multiple sources in the same domain. In *International Conference on Learning Representations*.

Clemens Rosenbaum, Ignacio Cases, Matthew Riemer, and Tim Klinger. 2019. Routing networks and the challenges of modular and compositional computation. *arXiv preprint arXiv:1904.12774*.

Sebastian Ruder, Joachim Bingel, Isabelle Augenstein, and Anders Søgaard. 2019. Latent multi-task architecture learning. In *Proceedings of the AAAI Conference on Artificial Intelligence*, pages 4822–4829.

Andrei A Rusu, Dushyant Rao, Jakub Sygnowski, Oriol Vinyals, Razvan Pascanu, Simon Osindero, and Raia Hadsell. 2019. Meta-learning with latent embedding optimization. In *International Conference on Learning Representations*.

Victor Sanh, Albert Webson, Colin Raffel, Stephen H. Bach, Lintang Sutawika, Zaid Alyafeai, Antoine Chaffin, Arnaud Stiegler, Teven Le Scao, Arun Raja, Manan Dey, M. Saiful Bari, Canwen Xu, Urmish Thakker, Shanya Sharma, Eliza Szczechla, Taewoon Kim, Gunjan Chhablani, Nihal V. Nayak, Debajyoti Datta, Jonathan Chang, Mike Tian-Jian Jiang, Han Wang, Matteo Manica, Sheng Shen, Zheng Xin Yong, Harshit Pandey, Rachel Bawden, Thomas Wang, Trishala Neeraj, Jos Rozen, Abheesht Sharma, Andrea Santilli, Thibault Févry, Jason Alan Fries, Ryan Teehan, Stella Biderman, Leo Gao, Tali Bers, Thomas Wolf, and Alexander M. Rush. 2022. Multitask prompted training enables zero-shot task generalization. In *The Tenth International Conference on Learning Representations*.

John Schulman, Philipp Moritz, Sergey Levine, Michael Jordan, and Pieter Abbeel. 2015. High-dimensional continuous control using generalized advantage estimation. *arXiv preprint arXiv:1506.02438*.

John Schulman, Filip Wolski, Prafulla Dhariwal, Alec Radford, and Oleg Klimov. 2017. Proximal policy optimization algorithms. *arXiv preprint arXiv:1707.06347*.

Noam Shazeer, Azalia Mirhoseini, Krzysztof Maziarz, Andy Davis, Quoc Le, Geoffrey Hinton, and Jeff Dean. 2017. Outrageously large neural networks: The sparsely-gated mixture-of-experts layer. In *International Conference on Learning Representations*.

Asa Cooper Stickland and Iain Murray. 2019. BERT and PALs: Projected attention layers for efficient adaptation in multi-task learning. In *Proceedings of the 36th International Conference on Machine Learning*, pages 5986–5995.

Tianxiang Sun, Yunfan Shao, Xiaonan Li, Pengfei Liu, Hang Yan, Xipeng Qiu, and Xuanjing Huang. 2020. Learning sparse sharing architectures for multiple tasks. In *Proceedings of the AAAI Conference on Artificial Intelligence*, volume 34, pages 8936–8943.

Richard Stuart Sutton. 1984. *Temporal credit assignment in reinforcement learning*. Ph.D. thesis, University of Massachusetts Amherst.

Alex Wang, Amanpreet Singh, Julian Michael, Felix Hill, Omer Levy, and Samuel Bowman. 2018. GLUE: A multi-task benchmark and analysis platform for natural language understanding. In *Proceedings of the 2018 EMNLP Workshop BlackboxNLP: Analyzing and Interpreting Neural Networks for NLP*, pages 353–355.

Zirui Wang, Yulia Tsvetkov, Orhan Firat, and Yuan Cao. 2021. Gradient vaccine: Investigating and improving multi-task optimization in massively multilingual models. In *International Conference on Learning Representations*.

Jason Wei, Maarten Bosma, Vincent Y Zhao, Kelvin Guu, Adams Wei Yu, Brian Lester, Nan Du, Andrew M Dai, and Quoc V Le. 2021. Finetuned language models are zero-shot learners. *arXiv preprint arXiv:2109.01652*.

Paul J Werbos. 1990. Backpropagation through time: what it does and how to do it. *Proceedings of the IEEE*, 78(10):1550–1560.

Yuhuai Wu, Elman Mansimov, Roger B Grosse, Shun Liao, and Jimmy Ba. 2017. Scalable trust-region method for deep reinforcement learning using kronecker-factored approximation. *Advances in neural information processing systems*, 30.

Qinyuan Ye, Bill Yuchen Lin, and Xiang Ren. 2021. CrossFit: A few-shot learning challenge for cross-task generalization in NLP. In *Proceedings of the 2021 Conference on Empirical Methods in Natural Language Processing*, pages 7163–7189.

Yanzhe Zhang, Xuezhi Wang, and Diyi Yang. 2022. Continual sequence generation with adaptive compositional modules. In *Proceedings of the 60th Annual Meeting of the Association for Computational Linguistics (Volume 1: Long Papers), ACL 2022, Dublin, Ireland, May 22-27, 2022*, pages 3653–3667. Association for Computational Linguistics.

# A Hyper-parameters

## A.1 BabyAI

We follow closely the best hyper-parameter setup of Hui et al. (2020). Tiles in the visual input are encoded into embeddings of size 128 via a look-up table. The CNN has 2 layers, filter size 3, stride 1, and padding 1; whereas the FiLM module has 2 layers. A residual layer is added between the CNN output and each of the FiLM layers. The output of FiLM is max-pooled with a layer of size 7 and stride 2. Both the LSTM and the GRU have a hidden size of 128.

A learning rate of 1e-4 is adopted for Adam (Kingma and Ba, 2015). We optimise the model with Proximal Policy Optimisation (PPO; Schulman et al., 2017) and Back-Propagation Through Time (BPTT; Werbos, 1990). Additionally, we use an Advantage Actor–Critic (A2C; Wu et al., 2017) with Generalised Advantage Estimation (GAE; Schulman et al., 2015). The reward is calculated as $(1-0.9\,n/n_{\max})$ if the agent completes a task—where $n$ is the number of steps required and $n_{\max}$ is a threshold set according to the level difficulty, 0 otherwise. Returns are discounted by $\gamma = 0.99$.

## A.2 CrossFit

During both multitask pre-training and few-shot adaptation, we use the Adam optimiser (Kingma and Ba, 2015) and select a learning rate for $\Phi$ among $\{1e-2, 1e-3, 1e-4\}$ based on performance on the development sets of $\mathcal{T}_{train}$ and $\mathcal{T}_{dev}$, respectively. As a more aggressive learning rate for $Z$ in SKILLED instead we search in the range $[1e-1, 1e-2]$. We run multitask pre-training for 30 epochs with an effective batch size of 32, with a warm-up of 6% of the total steps. Instead, during few-shot adaptation, the effective batch size is 8 for 1000 training steps, with a warm-up rate of 10% and a weight decay of 1e-2. For each held-out task, a newly added row in $Z$ (initialised with a vector of 0.5) and $\Phi$ (initialised from pre-training) are fine-tuned, but not $\vartheta_0$.

For a comparison of parameter counts, LoRA adds $4l(2hr + |\mathcal{T}|) \cdot |\mathcal{S}|$ parameters to the pre-trained model, where $l$ is the number of layers in the encoder and decoder, $h$ is the hidden size, and 4 is the number of linear projections in self-attention (query, key, value, output). We use $r = 16$, $l = 24$ and $h = 1024$ for BART Large, so we add $\sim 3 \cdot 10^6$ parameters per skill. Given that the pre-trained model has $\sim 4 \cdot 10^8$ parameters, this implies an increase of $\sim 0.78\%$ per skill. HYPER adds $4l(2he + 2e) \cdot e$ parameters, an increase of $\sim 0.78\%$ per task embedding dimension.

# B Additional Results for BabyAI

| Skills | Level |
|---|---|
| 1 2 3 4 8 | GOTO |
| 1 8 | GOTOOBJMAZE |
| 1 2 3 6 7 | PICKUPLOC |
| 1 2 3 5 | PUTNEXTLOCAL |
| 1 2 3 4 | GOTOLOCAL |
| 1 2 3 | GOTOREDBALL |
| 1 2 | GOTOREDBALLGREY |
| 1 | GOTOOBJ |

Table 2: BabiAI EXPERT task–skill allocation.

| Model | Episodes |
|---|---|
| PRIVATE | >6000000 |
| SHARED | 3544294 |
| EXPERT | 4608019 |
| SKILLED | **2218226** |
| - SPARSITY | 1853060 |

Table 3: Sample efficiency of various models on 8 BabyAI levels measured as the number of episodes needed to reach a success rate $> 0.99$.

# C Additional Results for CrossFit

| Metric | SHARED | HYPER | SKILLED |
|---|---|---|---|
| TASK-SPECIFIC | | | |
| Acc | 58.47 | 62.63 | 62.66 |
| C-F1 | 41.76 | 56.74 | 55.39 |
| EM | 20.05 | 21.68 | 21.70 |
| P-Corr | 56.83 | 61.54 | 52.60 |
| QA-F1 | 48,88 | 51.04 | 52.35 |
| Rouge-L | 28.02 | 26.71 | 28.05 |
| GLOBAL | | | |
| Average | 43.09 | 49.37 | 48.95 |

Table 4: Performance of multitask models averaged over test sets of 120 seen CrossFit task. Performance is both aggregated globally across all tasks (in terms of task-specific metrics) and across subsets of tasks with the same evaluation metric.

| | |
|---|---|
| | ELI5-ASKS, ELI5-ELI5, ETHOS-SEXUAL-ORIENTATION |
| 3 | GOOGLE-WELLFORMED-QUERY, REDDIT-TIFU-TITLE |
| 2 | APP-REVIEWS, CLIMATE-FEVER, DBPEDIA-14, EMOTION, GLUE-MRPC, GLUE-RTE, GLUE-SST2, GLUE-WNLI, HATEXPLAIN, IMDB, LIAR, MOCHA, ONESTOP-ENGLISH, PAWS, PIQA, POEM-SENTIMENT, ROTTEN-TOMATOES, SCICITE, TAB-FACT, TREC-FINEGRAINED, TWEET-EVAL-EMOJI, TWEET-EVAL-SENTIMENT, TWEET-EVAL-STANCE-ABORTION, TWEET-EVAL-STANCE-ATHEISM, TWEET-EVAL-STANCE-CLIMATE, TWEET-EVAL-STANCE-FEMINIST, WIKI-AUTO, YAHOO-ANSWERS-TOPICS, YELP-REVIEW-FULL |
| 2 3 | ADE-CORPUS-V2-DOSAGE, BIOMRC, BOOLQ, EMO, ETHOS-DISABILITY, HATE-SPEECH18, KILT-AY2, LAMA-CONCEPTNET, LAMA-GOOGLE-RE, LAMA-SQUAD, MC-TACO, NUMER-SENSE, PROTO-QA, ROPES, SEARCH-QA, SMS-SPAM, SUPERGLUE-RECORD, TWEET-EVAL-HATE, TWEET-EVAL-IRONY, TWEET-EVAL-OFFENSIVE |
| 1 | CIRCA, CRAWL-DOMAIN, GLUE-COLA, SUPERGLUE-RTE |
| 1 3 | LAMA-TREX, LIMIT, QA-SRL, SUPERGLUE-MULTIRC, TWEET-EVAL-STANCE-HILLARY, WIKISQL |
| 1 2 | AI2-ARC, ANLI, AQUA-RAT, BLIMP-SENTENTIAL-NEGATION-NPI-LICENSOR-PRESENT, CODAH, ETHOS-GENDER, ETHOS-NATIONAL-ORIGIN, ETHOS-RACE, ETHOS-RELIGION, FREEBASE-QA, GLUE-MNLI, GLUE-QQP, HELLASWAG, MEDICAL-QUESTIONS-PAIRS, OPENBOOKQA, QUAREL, QUARTZ-NO-KNOWLEDGE, QUARTZ-WITH-KNOWLEDGE, RACE-MIDDLE, SCITAIL, SICK, SOCIAL-I-QA, SUPERGLUE-CB, SUPERGLUE-COPA, SUPERGLUE-WIC, SUPERGLUE-WSC, SWAG, WIKI-QA |
| 1 2 3 | ADVERSARIALQA, ART, COMMONSENSE-QA, COS-E, DEFINITE-PRONOUN-RESOLUTION, ETHOS-DIRECTED-VS-GENERALIZED, HOTPOT-QA, SCIQ, SQUAD-WITH-CONTEXT, WINO-GRANDE, WIQA |
| 0 | BREAK-QDMR, BREAK-QDMR-HIGH-LEVEL, E2E-NLG-CLEANED, ELI5-ASKH, MULTI-NEWS |
| 0 3 | AESLC, COMMON-GEN, GIGAWORD, RACE-HIGH, REDDIT-TIFU-TLDR, TWEET-QA, WIKI-SPLIT |
| 0 2 | AG-NEWS, KILT-WOW |
| 0 2 3 | BLIMP-SENTENTIAL-NEGATION-NPI-SCOPE, DISCOVERY, HATE-SPEECH-OFFENSIVE, JEOPARDY, KILT-HOTPOTQA, KILT-NQ, KILT-TREX, KILT-ZSRE, SQUAD-NO-CONTEXT, WEB-QUESTIONS, XSUM |
| 0 1 | ADE-CORPUS-V2-CLASSIFICATION, ASLG-PC12, FINANCIAL-PHRASEBANK, GLUE-QNLI, SPIDER |
| 0 1 3 | SAMSUM, TREC, WIKI-BIO |
| 0 1 2 | AMAZON-POLARITY, BLIMP-ANAPHOR-GENDER-AGREEMENT, BLIMP-ANAPHOR-NUMBER-AGREEMENT, BLIMP-DETERMINER-NOUN-AGREEMENT-WITH-ADJ-IRREGULAR-1, BLIMP-ELLIPSIS-N-BAR-1, BLIMP-ELLIPSIS-N-BAR-2, BLIMP-EXISTENTIAL-THERE-QUANTIFIERS-1, BLIMP-IRREGULAR-PAST-PARTICIPLE-ADJECTIVES, BLIMP-WH-QUESTIONS-OBJECT-GAP, COSMOS-QA, CROWS-PAIRS, DREAM, KILT-FEVER, MATH-QA, QUOREF |
| 0 1 2 3 | ACRONYM-IDENTIFICATION, ADE-CORPUS-V2-EFFECT, DUORC, EMPATHETIC-DIALOGUES, HEALTH-FACT, QASC, QUAIL, TWEET-EVAL-EMOTION, YELP-POLARITY |

Table 5: Skill allocation to 120 training CrossFit tasks for $|\mathcal{S}| = 4$.

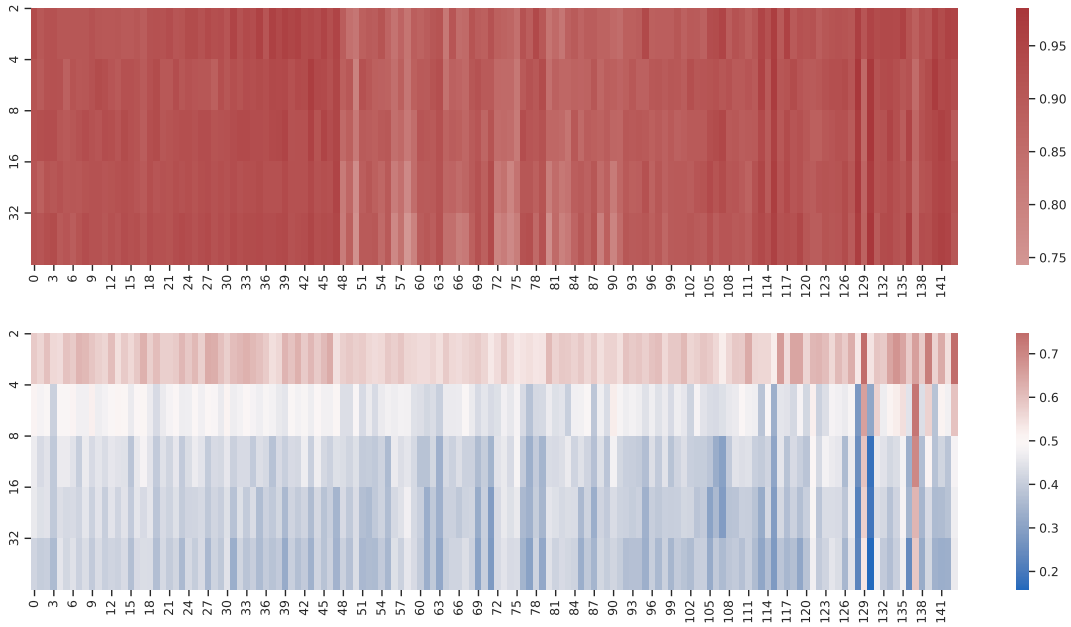

Figure 6: Per-layer discreteness (top) and per-layer sparsity (bottom).

## D Additional In-Depth Analysis of Learned Skills

Specifically, we measure:

1. *Discreteness*. How close is the continuous relaxation to a binary matrix? To this end, we report the average normalised entropy across all probabilities in the cells of the matrix:

$$\text{Discrete}(Z) = \frac{1}{|\mathcal{T}| \cdot |\mathcal{S}|} \sum_{\mathcal{T}_i} \sum_{\mathcal{S}_j} \frac{\mathcal{H}(z_{ij})}{\log 2} \quad (5)$$

   For instance, a binary matrix yields a score of 1, a matrix where every cell is 0.5 a score of 0.

2. *Sparsity*. How many skills are active per task on average? We count the rate of non-zero cells in the values rounded to the closest integer:

$$\text{Sparsity}(Z) = \frac{1}{|\mathcal{T}| \cdot |\mathcal{S}|} \sum_{\mathcal{T}_i} \sum_{\mathcal{S}_j} \lfloor z_{ij} \rceil \quad (6)$$

3. *Usage*. Is the allocation of skills across tasks balanced or are some preferred over others? We provide the normalised entropy of a categorical distribution parameterised by $\sum_j Z_{\star,j}$, the sum of the columns of $Z$:

$$\text{Usage}(Z) = \frac{\mathcal{H}\left[\sum_{\mathcal{T}_i} z_{i,\star}\right]}{\log |\mathcal{S}|} \quad (7)$$

Note that the entropy values are normalised into the range $[0, 1]$ to make them invariant to the number of skills: this quantity is known as 'efficiency'.

We plot these metrics—as well as the performance on in-domain train tasks in terms of exact match—as a function of the skill inventory size in Figure 7. We find that, whilst a continuous relaxation, the learned matrices are highly discretised and all their values are extremely close to either 0 or 1. Moreover, the level of sparsity decreases as the number of skills increases. This means that relatively smaller subsets of skills are required. Instead, usage stays consistently near the maximum value, which implies that there is uniformity in how frequently each skill is active across tasks. Finally, exact match is consistently high for sufficiently large ($|\mathcal{S}| \geq 8$) skill inventories.

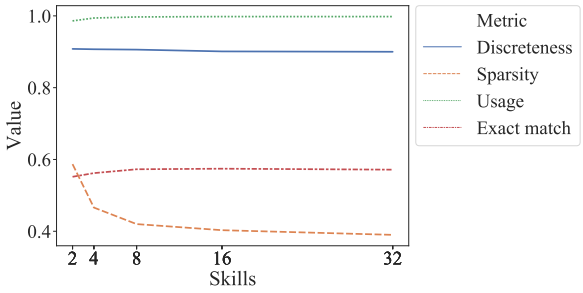


Figure 7: Statistics of the task–skill matrices for different choices of skill inventory size, including: discreteness, sparsity, usage, and the average exact match on the development set of 120 CrossFit tasks.